Regularized DFA to study the gaze position of an airline pilot

Bastien Berthelot*†, Éric Grivel‡, Pierrick Legrand†, Jean-Marc André‡ and Patrick Mazoyer*

* THALES AVS France, Campus THALES Bordeaux/THALES Toulouse
† Bordeaux University - IMB UMR CNRS 5251 - INRIA, FRANCE
‡ Bordeaux University - INP Bordeaux - IMS - UMR CNRS 5218, FRANCE

***Abstract*—To estimate the Hurst exponent of a mono-fractal process, the detrended fluctuation analysis (DFA) is based on the estimation of the trend of the integrated process. The latter is subtracted from the integrated process. The power of the residual is then computed and corresponds to the square of the fluctuation function. Its logarithm is proportional to the Hurst exponent. In the last few years, a few variants of this method have been proposed and differ in the way of estimating the trend. Our contribution in this paper is threefold. First, we introduce a new variant of the DFA, based on a regularized least-square criterion to estimate the trend. Then, the influence of the regularization parameter on the fluctuation function is analyzed in two cases: when the process is wide sense stationary and when it is not. Finally, an application is presented in the field of aeronautics to characterize an attentional impairment: the visual tunneling.**

***Index Terms*—filter, interpretation, Hurst, DFA**

I. Introduction

In order to characterize the evolution of a given signal, it is usual to extract a set of parameters. This can be done in the time domain, in the frequency domain, etc. For example, when dealing with a mono-fractal process, the Hurst exponent can be computed to quantify its long range memory. In the last few years, a great deal of interest has been paid to robust estimators of the Hurst exponent. To cite a few[1], the wavelet based analysis [1], the empirical mode decomposition [13] and the methods based on the estimation of the trend of the process have been proposed. The latter are addressed in this paper, as they usually provide an accurate estimation the Hurst exponent while remaining simple to use for the practitioner. Among the pioneering works, the detrended fluctuation analysis (DFA) was proposed in 1994 [9]. The DFA operates with the following steps: the signal of length M is first centered and integrated, leading to what is called the *profile*. Then, its trend has to be estimated. Peng *et al.* suggest splitting the profile into L non-overlapping parts of length N, where L is the integer part of $\frac{M}{N}$. The frame trends corresponding to segments are estimated and concatenated to get the trend of the whole profile. The latter is then removed from the profile, to obtain the residual. The residual power, denoted as $F^2(N)$, is computed for different values of N. Studying this quantity is of interest because the evolution of $\log(F(N))$ as a function of $\log(N)$ has been shown to be linear, with the slope α linked the Hurst exponent H as follows: $\alpha = H + 1$.

[1]The reader may refer to [3] for a more exhaustive state of the art.

The variants of the DFA mainly differ in the way of detrending the process. Thus, in the detrending moving average (DMA) method [2], the trends are deduced from the profile as the result of its filtering by a causal finite-impulse low-pass filter of order N. Non-causal or infinite-impulse response filters have been also designed. See [18] for more details. In addition, when the DFA is used, discontinuities in the global trend necessarily appear every N samples while the profile does not have any. As this can bring unwanted artifacts in the residual, Riley *et al.* developed the adaptive fractal analysis (AFA) [12] while we recently proposed the continuous DFA (CDFA) [3], where the trend is a set of continuous segments.

In this paper, our contributions are threefold:

1) we propose a new variant of the DFA, the purpose of which is to reduce the discontinuities that appear in the global trend. It is based on the Tikhonov regularization and amounts to considering Hodrick-Prescott filtering [6]. This type of regularization approaches has already been used in applications such as biomedical signal analysis and econometrics. Thus, it was applied to detrend heart rate processes in [17] by Tarvainen *et al.*, to remove unwanted low frequency components from processes in order to estimate physiological parameters [10], or to detect stress [5]. In the present work, instead of using this well-established approach to filter a given process, we employ it to create a variant of the DFA, called regularized DFA (RDFA).

2) we study the influence of the regularization parameter on the fluctuation function. For this purpose, we take advantage of the formalism we introduced in [3] and [4] to address both wide-sense stationary and non-stationary processes.

3) we analyze its relevance on the gaze position of an airline pilot to characterize the visual tunneling (VT) state.

The remainder of the paper is organized as follows: in section II, our new variant is presented. Section III deals with the influence of the regularization parameter λ on the square of the fluctuation function. Section IV is about the use of the RDFA in aeronautics.

II. Regularized DFA

Before presenting the different steps of the RDFA in a matrix formulation, some notations must be introduced:

- $\mathbb{0}_{j\times k}$ is a matrix of size $j \times k$ filled with zeros whereas $\mathbb{1}_{1\times j}$ is a vector of size $1 \times j$ filled with ones.

- I_j is the identity matrix of size $j \times j$.
- $diag([.], j)$ is a matrix whose elements of the j^{th} diagonal are the vector $[.]$.

Let us consider Y the column vector storing the M samples of the signal, *i.e.* $\{y(n)\}_{n=1,...,M}$. Centering and integrating the signal leads to the column vector Y_{int} which satisfies:

$$Y_{int} = [y_{int}(1), y_{int}(2), ..., y_{int}(M)]^T = \mathrm{H}_M J_M Y \quad (1)$$

with:

$$\begin{cases} J_M = I_M - \frac{1}{M}\mathbb{1}_{M\times M} \\ H_M = \sum_{r=0}^{M-1} diag(\mathbb{1}_{1\times M-r}, -r) \end{cases} \quad (2)$$

H_M is hence a lower triangular matrix filled with 1s.
As M is not necessarily a multiple of N, the last $M - LN$ samples of the profile are not taken into account. This amounts to pre-multiplying Y_{int} by $C = [I_{LN} \quad \mathbb{0}_{LN\times(M-(LN))}]$. Thus, one has:

$$\begin{aligned} Y_{int}(1:LN) &= [y_{int}(1), y_{int}(2), ..., y_{int}(LN)]^T \quad (3) \\ &= CY_{int} \underset{(1)}{=} C\mathrm{H}_M J_M Y \end{aligned}$$

As done in [9], let us decompose $Y_{int}(1 : LN)$ into L non-overlapping vectors of length N. For the l^{th} one, with $l = 1, ..., L$, let us search for the trend vector T_l of size $N \times 1$. If a straight line of the form $a_{l,1}[(l-1)N+n]+a_{l,0}$ is chosen to model the local trend, one has:

$$T_l = A_l \theta_l \quad (4)$$

where A_l is a $N \times 2$ matrix whose first column corresponds to a vector of 1 and whose second column is defined by the set of values $\{(l-1)N+n\}_{n=1,...,N}$ and $\theta_l = \begin{bmatrix} a_{l,0} & a_{l,1} \end{bmatrix}^T$. In the following, given A the $LN \times 2L$ block diagonal matrix defined from the set of matrices $\{A_l\}_{l=1,...,L}$ and Y_{int}, our purpose is to estimate $\Theta = \begin{bmatrix} \theta_1^T \dots \theta_L^T \end{bmatrix}^T$ the parameter vector of size $2L \times 1$. For this purpose, the Tikhonov regularization can be considered. It consists in minimizing the following criterion:

$$\arg\min_{\Theta} \{||CY_{int} - A\Theta||^2 + \lambda^2 ||D_2 A\Theta||^2\} \quad (5)$$

where $||CY_{int} - A\Theta||^2$ corresponds to the power of the residual and λ is a regularization parameter. In addition, as the 2^{nd}-derivative operator D_2 of size $(LN-2) \times LN$ is defined by:

$$D_2 = \begin{bmatrix} 1 & -2 & 1 & \cdots & 0 \\ \vdots & \ddots & \ddots & \ddots & \vdots \\ 0 & \cdots & 1 & -2 & 1 \end{bmatrix}, \quad (6)$$

$D_2 A\Theta$ is a column vector of length $LN-2$ which corresponds to the second-order derivative of the global trend. Therefore, $||D_2 A\Theta||^2$ is null when the global trend is continuous, but can take large values when the global trend exhibits discontinuities.

The criterion (5) can be rewritten as follows:

$$\arg\min_{\Theta} \left\{ \left|\left| \begin{bmatrix} A \\ \lambda D_2 A \end{bmatrix} \Theta - \begin{bmatrix} CY_{int} \\ \mathbb{0}_{(LN-2)\times 1} \end{bmatrix} \right|\right|^2 \right\} \quad (7)$$

If $L^{ext} = \begin{bmatrix} I_{LN} & \mathbb{0}_{(LN-2)\times 2L} \end{bmatrix}$, $A^{ext} = \begin{bmatrix} A \\ I_{2L} \end{bmatrix}$ and $Y_{int}^{ext} = \begin{bmatrix} CY_{int} \\ \mathbb{0}_{2L\times 1} \end{bmatrix}$, this amounts to considering the following criterion:

$$\arg\min_{\Theta} \left\{ \left|\left| L^{ext} A^{ext} \Theta - L^{ext} Y_{int}^{ext} \right|\right|^2 \right\} \quad (8)$$

for which the solution is given by:

$$\begin{aligned} \hat{\Theta}_\lambda &= \left({A^{ext}}^T {L^{ext}}^T L^{ext} A^{ext} \right)^{-1} {A^{ext}}^T {L^{ext}}^T L^{ext} Y_{int}^{ext} \quad (9) \\ &= \left(A^T A + \lambda^2 A^T D_2^T D_2 A \right)^{-1} A^T C \mathrm{H}_M J_M Y \end{aligned}$$

Remark: When $\lambda = 0$, the trend vector obtained with the DFA is retrieved. It corresponds to the orthogonal projection of $C\mathrm{H}_M J_M Y$ onto the space spanned by the columns of A. At this stage, the residual vector can be deduced and satisfies:

$$\begin{aligned} R_\lambda &= C\mathrm{H}_M J_M Y - A\hat{\Theta}_\lambda \quad (10) \\ &= \left(I_{LN} - A \left(A^T A + \lambda^2 A^T D_2^T D_2 A \right)^{-1} A^T \right) C\mathrm{H}_M J_M Y \end{aligned}$$

By considering the operator B_λ defined by $I_{LN} - A \left(A^T A + \lambda^2 A^T D_2^T D_2 A \right)^{-1} A^T$, one has:

$$R_\lambda = B_\lambda C\mathrm{H}_M J_M Y \quad (11)$$

The next step consists in expressing the square of the fluctuation function. By introducing the following $M \times M$ matrix:

$$\Gamma_\lambda = \frac{1}{LN} J_M^T \mathrm{H}_M^T C^T B_\lambda^T B_\lambda C \mathrm{H}_M J_M \quad (12)$$

and by using the properties of the trace of a matrix, the power of the residual $F_\lambda^2(N)$ can be expressed as:

$$F_\lambda^2(N) = Tr(\Gamma_\lambda Y Y^T) \quad (13)$$

As done in [9], $\log(F_\lambda(N))$ is plotted as a linear function of $\log(N)$. The goal is to search a straight line fitting the log-log representation. The quantity α is its slope and is estimated in the least-square sense. As α is computed from the log of $F_\lambda^2(N)$ for multiple values of N, it is a non-linear function of Y. Finally, the Hurst exponents H is equal to $\alpha - 1$.
In the following, using this matrix representation, let us analyze how λ impacts the RDFA for wide sense stationary (w.s.s.) processes, and more generally, for any type of processes.

III. Analysis of the influence of λ

A. When the signal is w.s.s.

In [3], we compared the DFA with the continuous DFA, were the global trend is constrained to be continuous. In both cases, the statistical mean of the square of the fluctuation function was expressed as a function of the correlation function and consequently as a function of the power spectral density of the signal. The fluctuation function is hence seen as the power of the signal filtered by a filter which varies from one method to another. This gave us the opportunity to study the differences between both methods. In this section, we propose to follow the same formalism in order to analyze the influence of the regularization parameter λ on the filtering induced by the RDFA.

1) Expressing the fluctuation function using the PSD of the signal: By assuming that y is w.s.s and taking the statistical mean of (13), one has:

$$E[F_\lambda^2(N)] = \sum_{r=-LN+1}^{LN-1} Tr(\Gamma_\lambda, r) R_{y,y}(r) \tag{14}$$

where $R_{y,y}(r)$ is the autocorrelation function of the process y and $Tr(\Gamma_\lambda, r)$ denotes the r^{th} diagonal of the matrix Γ_λ. Given the Wiener-Khintchine theorem and using the inverse Fourier transform (TF^{-1}), $E[F_\lambda^2(N)]$ can be expressed from the PSD of y, denoted as $S_{yy}(f)$:

$$\begin{aligned} E[F_\lambda^2(N)] &= TF^{-1}\Big(\big(\sum_{r=-LN+1}^{LN-1} Tr(\Gamma_\lambda(r) e^{-j2\pi f_n r} \big) S_{yy}(f) \Big)\Big|_{\tau=0} \\ &= TF^{-1}\Big(\Psi_\lambda(f) S_{yy}(f) \Big)\Big|_{\tau=0} \end{aligned} \tag{15}$$

$\Psi_\lambda(f) S_{yy}(f)$ is the PSD of the signal y filtered by a filter whose transfer function $H_\lambda(z)$ satisfies:

$$\Psi_\lambda(f) = |H_\lambda(z)|^2_{z=exp(j\theta)} \tag{16}$$

with $\theta = 2\pi f / f_s$ the normalized angular frequency. Consequently, $E[F_\lambda^2(N)]$ corresponds to the autocorrelation function of the filter output calculated for the lag equal to 0, *i.e.* the power of the filter output. In what follows, we propose to study the influence of λ on $\Psi_\lambda(f)$.

2) Influence of λ on the filtering: Let us first look at the two examples provided in Fig. 1a and 1b where the cases $N = 3$ and $N = 5$ are pictured. The larger λ, the more the filter acts as a band-pass filter, and the spikier its resonance. In addition, it appears that $\Psi_\lambda(f)$ is an increasing function of λ. Let us quantify the degrees of similarity between the RDFA and the DFA when N increases. One objective way to compare $\Psi_\lambda(f)$ with $\Psi_0(f)$ is to compute their log spectral distance (LSD) [11]. The smaller the LSD, the more similar both spectra. The evolution of the LSD as a function of $\log(N)$ is depicted in Fig. 2 for different values of λ. For each value of λ, the LSD decreases when N increases. In addition, for a given value of N, the smaller λ, the smaller the LSD.

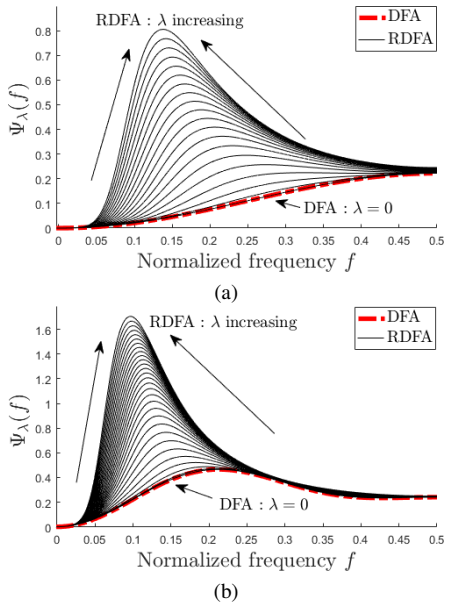

Figure 1: (a) $\Psi_\lambda(f)$ for $N = 3$, when λ increases from 0, *i.e.* the DFA case, to 2 with a step of 0.1; (b) $\Psi_\lambda(f)$ for $N = 5$, when λ increases from 0 to 3 with a step of 0.1.

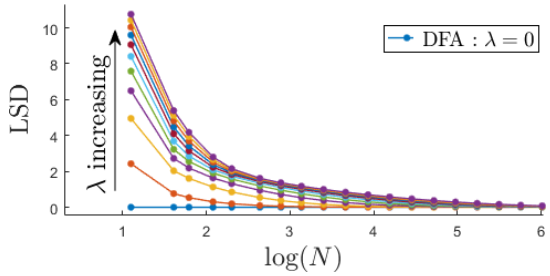

Figure 2: Evolution of the LSD between $\Psi_\lambda(f)$ and $\Psi_0(f)$ as a function of $\log(N)$, with λ between 0 and 5.

3) Influence of λ on the fluctuation function: Given the above comments, when studying a w.s.s. process, the values of $\log(F_\lambda(N))$ obtained with the RDFA ($\lambda > 0$) are larger than the ones obtained with the DFA ($\lambda = 0$) for any N. The resulting curves are necessarily one above the other when λ increases but they are not parallel because the LDSs decay and converge towards zero when N increases. To illustrate this phenomenon, let us apply the RDFA on 150 realizations of a white Gaussian noise, for which the expected value of α is 0.5. When the DFA is used, as illustrated in [7], the mean of $\log(F_0(N))$ is under-evaluated when N is small. This corresponds to a shifted point in Fig 3.

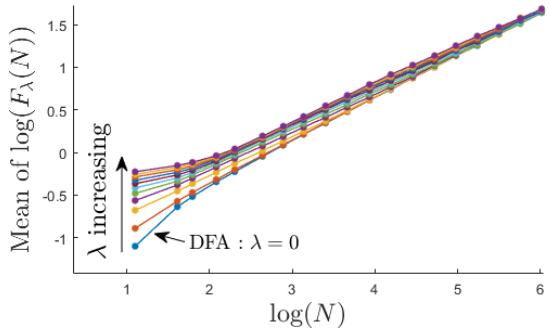

Figure 3: Evolution of the mean of $\log(F_\lambda(N))$ vs. $\log(N)$, estimated on 150 white noises.

As a consequence, the estimation of α with the DFA is altered and tends to be overevaluated. Using a small value of λ makes it possible to weaken this phenomenon. However, a too large value can have the opposite effect, as shown in Table I.

λ	$\lambda = 0$	$\lambda = 0.5$	$\lambda = 1$	$\lambda = 5$
Mean of α on 150 realizations	0.537	0.508	0.468	0.410

Table I: Mean values of α obtained with different values of λ

In many cases, the signal is not necessarily w.s.s. For this reason, we propose to analyze the general case in the next section.

B. When the signal is not w.s.s.

In [4], the DFA and the DMA were analyzed. The square of the fluctuation function was expressed as a 2D Fourier transform (2D-FT) of the product of two matrices. The first one was defined from the instantaneous correlations of the signal while the second, called the weighting matrix, differed from one method to another. Analyzing the properties of the 2D-FT of the weighting matrix is hence useful to highlight the differences between the methods. Here, the same procedure is used to analyze the impact of the regularization parameter.

1) Expression of the square of fluctuation function: As M is the size of the square matrix Γ_λ, (13) becomes:

$$F^2_\lambda(N) = \sum_{k=1}^{M} \Gamma_\lambda(k,k)y^2(k) + \sum_{r=1}^{M-1}\sum_{k=1}^{M-r} [\Gamma_\lambda(k,k+r)+\Gamma_\lambda(k+r,k)]y(k)y(k+r) \quad (17)$$

where $\{y(k)y(k+r)\}_{r=-M+1,\ldots,M-1}$ can be seen as instantaneous correlations. The latter can be stored in the $(2M-1)\times(2M-1)$ matrix Y_{corr} whose element at the i^{th} row and j^{th} column is equal to $y(i)y(i+j-M)$. Following the same reasoning as in [4], (17) can be rewritten as a two-dimensional Fourier transform (2D-FT) of a matrix product:

$$\begin{aligned} F^2_\lambda(N) &= \mathscr{F}(Y_{corr}W_\lambda)|_{(u=0,v=0)} \\ &= \Big(\mathscr{F}(Y_{corr}) \circledast \mathscr{F}(W_\lambda)\Big)|_{(u=0,v=0)} \end{aligned} \quad (18)$$

where W_λ is a weighted matrix defined from the elements of Γ_λ, u and v are the normalized spatial frequencies, $\mathscr{F}$ denotes the 2D-FT and $\circledast$ the convolution.

Studying the impact of λ on the RDFA amounts to comparing the properties of the 2D-FT of W_λ. In the following, we focus our attention on $\log(|\mathscr{F}(W_\lambda|)$.

2) Analysis of the influence of the regularization parameter in the RDFA approach: The regularization parameter has an impact on $\log(|\mathscr{F}(W_\lambda|)$, and so on the way the RDFA acts on a non-w.s.s. process.

Let us first look at the influence of N on $\log(|\mathscr{F}(W_\lambda)|)$ for a given value of λ in Fig. 4. When N increases, the frequency content located at $u=0$ exhibits two mains lobes that shift towards low frequencies. This result is coherent with the analysis we had on $\Psi_\lambda(f)$ in the previous section. In addition, the large values of $\log(|\mathscr{F}(W_\lambda)|)$ are obtained for spatial frequencies that move more and more towards $(u,v)=(0,0)$. However, $|\mathscr{F}(W_\lambda)|_{(u=0,v=0)}$ remains close to 0, which confirms the detrending.

Let us now analyze the influence of λ for a given value of N. $\log(|\mathscr{F}(W_0)|)$ presents secondary lobes located at $u=\pm\frac{j}{N}$, $j=0,\ldots,\frac{N-1}{2}$. When $\lambda\neq 0$, most of them tend to lessen when λ increases. For $N=21$, λ which is at least equal to 5 is large enough to reduce the secondary lobes. As a consequence, one can expect a small difference between $F^2_0(21)$ and $F^2_{10}(21)$.

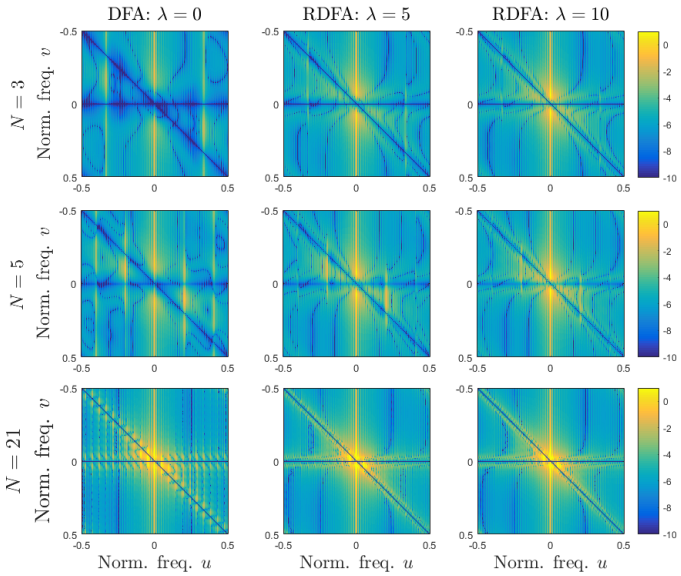

Figure 4: $\log(|\mathscr{F}(W_\lambda)|)$ with $\lambda=0$ (left), $\lambda=5$ (center) and $\lambda=10$ (right) for $N=\{3,5,21\}$.

C. Preliminary conclusion

Given the above analysis, the RDFA stands as an alternative to the DFA, especially when small values of N are used and as long as λ is not too large. In the next section, we propose to illustrate these works on real processes.

IV. Application

Our purpose is to analyze the regularity of an airline-pilot gaze position for the detection of the visual tunneling (VT) state. This cognitive state is defined as the inability for an individual to perceive an unexpected change in the visual scene [16]. It is a major factor of accidents in specific areas [15] and thus has been widely studied in the last fifteen years [8]. Our experiments aim at eliciting VT occurrences, by bringing different levels of mental workload and engagement into specific tasks.

For this reason, thirteen[2] subjects used a modified version of the multitasking simulator NASA MATB-II software [14], for its recognized similarities with pilot activities. For each subject, the gaze positions along both x and y-axis were collected from an eye-tracker[3].

A situation was labelled as VT if the following condition was met: no reaction to visual alarms, nor to secondary tasks, for a duration of more than twenty seconds. Thus, during our experiments, after spending a period of nominal activity (labelled *Nom*), eight out of the thirteen subjects underwent VT. Two of them experienced this phenomenon twice. So, ten cases of VT were identified.

For each of the forty processes[4] of length $M=800$,

[2]due to implementation constraints: piloting experience, neither glasses nor contact lenses allowed, etc.

[3]VT2 model from the company EyeTech, with a sampling rate at 40Hz.

[4]ten occurrences $\times$ two labels $\times$ two type of processes (gaze position along the x and y-axis).

the value of α is estimated with the DFA and the RDFA, with $\lambda = 1$. Note that referring to (5), for any $N > 3$, $||CY_{int} - A\hat{\Theta}_\lambda||^2\big|_{\lambda=1} > \lambda^2 ||D_2 A\hat{\Theta}_\lambda||^2\big|_{\lambda=1}$.
As presented in section II, $\log(F_\lambda(N))$ is plotted as a function of $\log(N)$. According to Fig. 5, where the mean and standard deviation values over all the processes are presented, the values of $\log(F_0(N))$ obtained for small values of N tend to increase the slope that would be induced by the set of values $\{\log(F_0(N))\}$ obtained when N is large. This phenomenon is weakened when $\lambda = 1$, especially in the VT case.

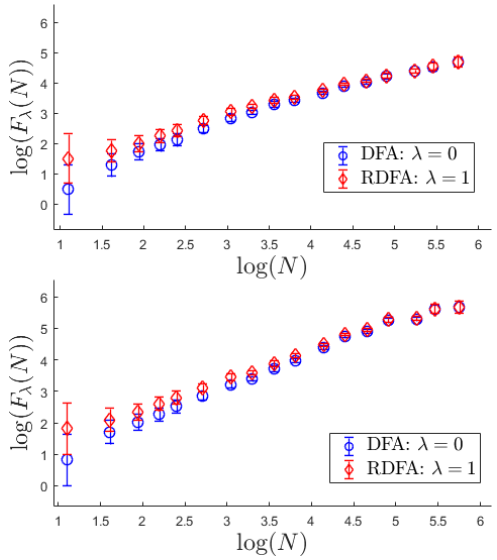

Figure 5: $\log(F_\lambda(N))$ vs. $\log(N)$, mean and standard deviation, for the VT (top), and *Nom* (bottom) cases.

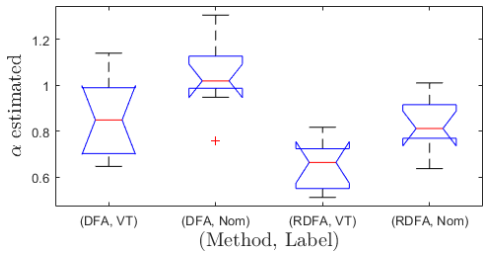

Figure 6: Value of α estimated on the gaze position along the x-axis with both the DFA and the RDFA.

Given Fig. 6, two comments can be made:

- No matter the estimation method used, there is a significant difference between the values of α obtained in the VT and the *Nom* cases. An ANOVA test conducted on these values provided the following p-values: $p_{DFA} = 0.025$ and $p_{RDFA} = 0.0032$. As a consequence, there is a correlation between the visual tunneling of a subject and the regularity of his gaze position along the x-axis. The RDFA appears to be more relevant than the DFA because the p-value is smaller.
- The estimation of α is lower with the RDFA, no matter the label. This is due to the compensation of $\log(F_\lambda(N))$ for small values of N, as depicted in Fig. 5.

V. Conclusion

A new variant of the DFA is proposed, based on a regularized estimation of the global trend. Our study reveals that the regularization parameter λ impacts the fluctuation function, especially on short time-scales, and thus can alleviate the bias induced by the DFA. As long as λ is not too large, the RDFA appears to be a relevant tool to detect the visual tunneling state of an aircraft pilot.

References

[1] P. Abry, P. Flandrin, M. S. Taqqu, and D. Veitch. Self-similarity and long-range dependence through the wavelet lens. *Theory and Applications of Long-range Dependence*, pages 527–556, 2003.

[2] E. Alessio, A. Carbone, G. Castelli, and V. Frappietro. Second-order moving average and scaling of stochastic time series. *The European Physical Journal B*, 27, 2:197–200, 2002.

[3] B. Berthelot, E. Grivel, P. Legrand, J.-M. André, P. Mazoyer, and T. Ferreira. Filtering-based Analysis Comparing the DFA with the CDFA for Wide Sense Stationary Processes. In *EUSIPCO 2019*, 2019.

[4] B. Berthelot, E. Grivel, P. Legrand, M. Donias, J.-M. André, P. Mazoyer, and T. Ferreira. 2D Fourier Transform Based Analysis Comparing the DFA with the DMA. In *EUSIPCO 2019* , 2019.

[5] J. Choi and R. Gutierrez-Osuna. Using heart rate monitors to detect mental stress. In *2009 Sixth International Workshop on Wearable and Implantable Body Sensor Networks*, pages 219–223, June 2009.

[6] R. J. Hodrick and E. C. Prescott. Postwar u.s. business cycles: An empirical investigation. *Journal of Money, Credit and Banking*, 29, (1):1–16, 1997.

[7] J. W. Kantelhardt, E. Koscielny-Bunde, H. H. A. Rego, S. Havlin, and A. Bunde. Detecting long-range correlations with detrended fluctuation analysis. *Physica A: Statistical Mechanics and its Applications*, 295, (3-4):441–454, 2001.

[8] K. Mathewson, G. Gratton, M. Fabiani, D. Beck, and T. Ro. To see or not to see: Prestimulus phase predicts visual awareness. *The Journal of neuroscience*, 29:2725–32, 04 2009.

[9] C. K. Peng, S. Buldyrev, S. Havlin, M. Simons, H. Stanley, and A. Goldberger. Mosaic organization of dna nucleotides. *Physical review. E*, 49:1685–9, 03 1994.

[10] M. Poh, D. J. McDuff, and R. W. Picard. Advancements in noncontact, multiparameter physiological measurements using a webcam. *IEEE Trans. on Biomedical Engineering*, 58(1):7–11, Jan 2011.

[11] L. R. Rabiner and B.-H. Juang. *Fundamentals of speech recognition*. PTR Prentice Hall, 1993.

[12] M. A. Riley, S. Bonnette, N. Kuznetsov, S. Wallot, and J. Gao. A tutorial introduction to adaptive fractal analysis. *Frontiers in Physiology*, 3:371, 2012.

[13] G. Rilling, P. Flandrin, and P. Gonçalves. Empirical mode decomposition, fractional gaussian noise and hurst exponent estimation. *International Conference on Acoustics, Speech and Signal Processing*, pages 489–492, 2005.

[14] Y. Santiago-Espada, R. R. Myer, K. A. Latorella, and J. R. Comstock. *The multi-attribute task battery ii (matb-ii) software for human performance and workload research: A user's guide*, 2011.

[15] S. Shappell and D. Wiegman. *A Human Error Analysis of General Aviation Controlled Flight Into Terrain Accidents Occurring Between 1990-1998*, 03 2003.

[16] D. J. Simons and C. F. Chabris. Gorillas in our midst: sustained inattentional blindness for dynamic events. *Perception*, pages 1059–1074, 1999.

[17] M. P. Tarvainen, P. O. Ranta-aho, and Pasi A. Karjalainen. An advanced detrending method with application to hrv analysis. *IEEE Trans. on Biomedical Engineering*, 49, 2:172–175, 2002.

[18] L. Xu, P. Ch. Ivanov, K. Hu, Z. Chen, A. Carbone, and H. E. Stanley. Quantifying signals with power-law correlations: A comparative study of detrended fluctuation analysis and detrended moving average techniques. *Physical Review E*, 71, 5:051101, 2005.